Available online at www.sciencedirect.com
ScienceDirect
Renewable Energy 33 (2008) 1911–1921
RENEWABLE ENERGY
www.elsevier.com/locate/renene

Analysis and design consideration of mean temperature differential Stirling engine for solar application

Iskander Tlili*, Youssef Timoumi, Sassi Ben Nasrallah

Laboratoire d'Etude des Systèmes Thermiques et Energétiques Ecole Nationale d'Ingénieurs de Monastir, Rue Ibn El Jazzar, 5019 Monastir, Tunisie

Received 17 August 2006; accepted 21 September 2007
Available online 5 November 2007

Abstract

This article presents a technical innovation, study of solar power system based on the Stirling dish (SD) technology and design considerations to be taken in designing of a mean temperature differential Stirling engine for solar application. The target power source will be solar dish/Stirling with average concentration ratio, which will supply a constant source temperature of 320 °C. Hence, the system design is based on a temperature difference of 300 °C, assuming that the sink is kept at 20 °C. During the preliminary design stage, the critical parameters of the engine design are determined according to the dynamic model with losses energy and pressure drop in heat exchangers was used during the design optimisation stage in order to establish a complete analytical model for the engine. The heat exchangers are designed to be of high effectiveness and low pressure-drop. Upon optimisation, for given value of difference temperature, operating frequency and dead volume there is a definite optimal value of swept volume at which the power is a maximum. The optimal swept volume of 75 cm^3 for operating frequency 75 Hz with the power is 250 W and the dead volume is of 370 cm^3.
© 2007 Elsevier Ltd. All rights reserved.

Keywords: Solar-powered; Stirling engine; Design; Losses; Regenerator; Thermal efficiency

1. Introduction

The harmony between environmental protection and economic growth has become a worldwide concern; there is an urgent need to effectively reuse solar energy, this source of energy is one of the more attractive renewable energy that can be used as an input energy source for heat engines. In fact, any heat energy source can be used with the Stirling engine. The solar radiation can be focused onto the heater of Stirling engine as shown in Fig. 1(a), thereby creating a solar-powered prime mover. The direct conversion of solar power into mechanical power reduces both the cost and complexity of the prime mover. In theory, the principal advantages of Stirling engines are their use of an external heat source and their high efficiency. Stirling engines are able to use solar energy that is a cheap source of energy.

Studies about high temperature Stirling engines have been extensively reported in the literature [1] and commercial units have been in operation for many years. On the other hand, low temperature Stirling engines are not as successful as their high temperature counterparts. However, the former have gained popularity in the last few decades due to this potential to tap a variety of low concentration energy sources available, such as solar. The increasing interest in Stirling engines is largely due to the fact the engine is more environmentally friendly than the widely used internal combustion engine, and also to its non-explosive nature in converting energy into mechanical form and thus leading to silent and cleaner operation, which are essential for special applications, such as military operations and medical uses.

The systems with very strong concentration [2] call upon an advanced and heavy technology, therefore are very expensive as they present, on the energy point of view, a limited interest. On the other hand, the systems without concentration are not economically viable. The best systems is with average concentration, leading to levels of temperature about 250–450 °C, but very few work seem to be devoted to the installations with average concentration. The company

*Corresponding author. Tel.: +216 98 61 97 04; fax: +216 73 50 05 14.
E-mail address: Iskander.Tlili@enim.rnu.tn (I. Tlili).

0960-1481/$ - see front matter © 2007 Elsevier Ltd. All rights reserved.
doi:10.1016/j.renene.2007.09.024

Nomenclature

A	area, m^2
C_p	specific heat at constant pressure, $J\,kg^{-1}\,K^{-1}$
C_{pr}	heat capacity of each cell matrix, $J\,K^{-1}$
C_v	specific heat at constant volume, $J\,kg^{-1}\,K^{-1}$
d	hydraulic diameter, m
D	diameter, m
dm	wire diameter, m
f_r	friction factor
Freq	operating frequency, Hz
h	convection heat transfer coefficient, $J\,m^{-2}\,s^{-1}\,K^{-1}$
J	annular gap between displacer and cylinder, m
k	thermal conductivity, $W\,m^{-1}\,K^{-1}$
L	length, m
M	mass of working gas in the engine, kg
$\dot{m}$	mass flow rate, $kg\,s^{-1}$
m	mass of gas in different component, kg
NTU	number of heat transfer unit
P	pressure, Pa
Q	heat, J
$\dot{Q}$	power, W
R	gas constant, $J\,kg\,K^{-1}$
T	temperature, K
V	volume, m^3
W	work, J

Subscripts

c	compression space
ch	load
d	expansion space
E	entered
ext	outside
f	cooler
h	heater
moy	mean
P	loss
Pa	wall
pis	piston
r	regenerator
$r1$	regenerator cell 1
$r2$	regenerator cell 2
S	left

Greek symbols

θ	crank angle, rad
ε	effectiveness
μ	Working GAS dynamic viscosity, $kg\,m^{-1}\,s^{-1}$
ρ	density, $kg\,m^{-3}$
ω	angular frequency, $rad\,s^{-1}$
ψ	mesh porosity

BSR Solar Technologies GmbH, which developed the SUNPULSE, also works on a system intended to produce electricity starting from solar energy fairly concentrated, which leads to levels of temperature about 450 °C.

Several analyses and simulation methods of the engine have been established [3], as well as the procedures for optimal design [4]. Most of the engines are fuel-fired and operate at high temperature, which highlights the need for careful material selection as well as good cooling system. For silent, light and portable equipment for leisure and domestic uses, low power engines may be more appropriate. Nevertheless, research in Stirling engine technology has been heavily masked by extensive and successful development of internal combustion engines, which have made Stirling engines less competitive. Hence, in order to design a low power engine using solar, new design specifications and optimisation criteria must be established [5–9]. This paper presents design considerations which may be taken to develop a solar Stirling engine with average concentration operating on mean temperature difference of 300 °C.

2. Losses in a Stirling engine

The energy losses in a Stirling engine are due to the thermodynamic and the mechanical processes. Compression and expansion are not adiabatic. The exchangers are not ideal since the pressure drops in the engine and the losses of heat in the exchangers exist. To accurately predict power and efficiency requires an understanding of the principle parasitic loss mechanisms.

2.1. Energy dissipation by pressure drops in heat exchangers $d\dot{Q}_{PCh}$

Pressure drops due to friction and to area changes in heat exchangers is given by [10]

$$\Delta p = -\frac{2f_r \mu G V}{A d^2 \rho}, \tag{1}$$

where G is working gas mass flow ($kg\,m^{-2}\,s^{-1}$), d is the hydraulic diameter, ρ is gas density ($kg\,m^{-3}$), V is volume (m^3) and f_r is the Reynolds friction factor.

The internal heat generation which occurs when the gas is forced to flow against the frictional drag force, is given by [10]:

$$d\dot{Q}_{Pch} = -\frac{\Delta p \dot{m}}{\rho}, \tag{2}$$

$\dot{m}$ is the mass flow rate ($kg\,s^{-1}$).

The total heat generated by pressure drop in the different exchangers is

$$d\dot{Q}_{PchT} = d\dot{Q}_{Pchf} + d\dot{Q}_{Pchr1} + d\dot{Q}_{Pchr2} + d\dot{Q}_{Pchh}. \tag{3}$$

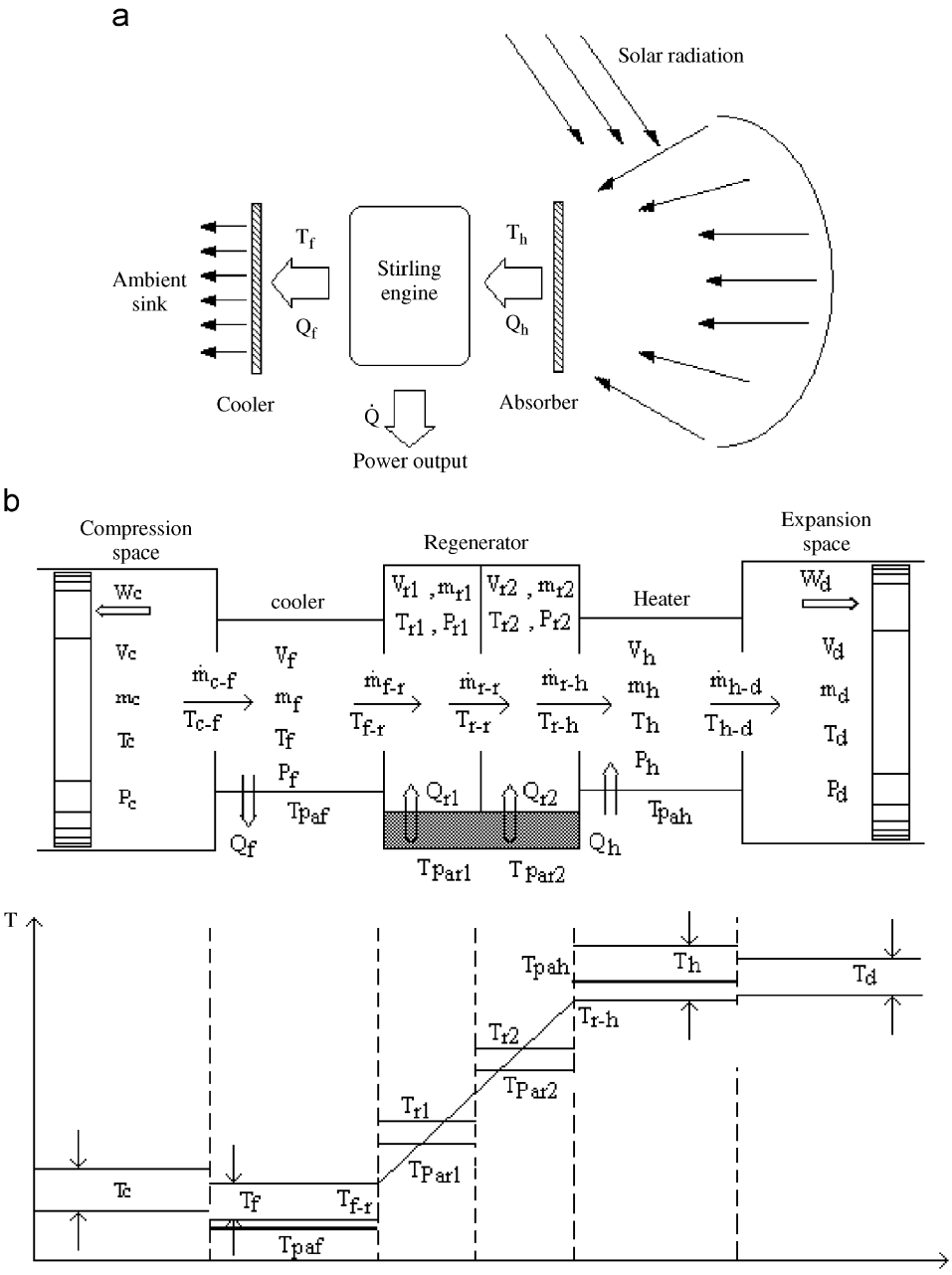

Fig. 1. (a) Schematic diagram of solar-powered Stirling engine. (b) Temperature distribution.

2.2. Energy lost by the internal conduction $\mathrm{d}\dot{Q}_{\mathrm{Pcd}}$

Energy lost due to the internal thermal conductivity between the hot parts and the cold parts of the engine through the exchangers are taken into account. These losses are directly proportional to the temperature difference at the ends of the exchanger; they are given for the different exchangers [11]:

$$\mathrm{d}\dot{Q}_{\mathrm{Pcdr}} = k_{\mathrm{cdr}} \frac{A_{\mathrm{r}}}{L_{\mathrm{r}}} (T_{\mathrm{r-h}} - T_{\mathrm{f-r}}), \tag{4}$$

$$\mathrm{d}\dot{Q}_{\mathrm{Pcdf}} = k_{\mathrm{cdf}} \frac{A_{\mathrm{f}}}{L_{\mathrm{f}}} (T_{\mathrm{f-r}} - T_{\mathrm{c-f}}), \tag{5}$$

$$\mathrm{d}\dot{Q}_{\mathrm{Pcdh}} = k_{\mathrm{cdh}} \frac{A_{\mathrm{h}}}{L_{\mathrm{h}}} (T_{\mathrm{h-d}} - T_{\mathrm{r-h}}), \tag{6}$$

k_{cd} ($\mathrm{W\,m^{-1}\,K^{-1}}$) is the material thermal conductivity; A is the effective area for conduction.

So the total conduction loss is:

$$\mathrm{d}\dot{Q}_{\mathrm{PcdT}} = \mathrm{d}\dot{Q}_{\mathrm{Pcdr}} + \mathrm{d}\dot{Q}_{\mathrm{Pcdf}} + \mathrm{d}\dot{Q}_{\mathrm{Pcdh}}. \tag{7}$$

2.3. Energy lost by external conduction $\mathrm{d}\dot{Q}_{\mathrm{Pext}}$

Energy lost by external conduction is considered in the regenerator which is not adiabatic. These losses are specified by the regenerator adiabatic coefficient, $\varepsilon \leqslant 1$,

definite as the report between the heat given up in the regenerator by the working gas at its passage towards the compression space and the heat received in the regenerator by the working gas at its passage towards the expansion space [10]. So the energy stored by the regenerator at the time of the passage of gas from the expansion space to the compression space is not completely restored with this gas at the time of its return.

For the ideal case of the regenerator perfected insulation, $\varepsilon = 1$.

The energy lost by external conduction is

$$d\dot{Q}_{Pext} = (1-\varepsilon)(d\dot{Q}_{r1} + d\dot{Q}_{r2}). \quad (8)$$

The effectiveness of the regenerator ε is given starting from the equation below [8]

$$\varepsilon = \frac{NTU}{1+NTU}, \quad (9)$$

NTU is the number of heat transfer unit:

$$NTU = \frac{hA_{wg}}{Cp\dot{m}}, \quad (10)$$

where h is the overall heat transfer coefficient (hot stream/matrix/cold stream), A_{wg} refers to the wall/gas, or "wetted" area of the heat exchanger surface, C_p the specific heat capacity at constant pressure, and $\dot{m}$ ($kg\,s^{-1}$) the mass flow rate through the regenerator.

2.4. Energy lost by Shuttle effect $d\dot{Q}_{Pshtl}$

Shuttling the displacer between hot and cold spaces within a machine introduces another mechanism for transferring heat from a hot to a cold space. Thus an important thermal effect appears in Stirling engines called 'Shuttle heat transfer' having the effect of increasing the apparent thermal conductance loss. The displacer absorbs a quantity of heat from the hot source and restores it to the cold source. This loss of energy is given by [11]:

$$d\dot{Q}_{Pshtl} = \frac{0.4Z^2 k_{pis} D_d}{JL_d}(T_d - T_c), \quad (11)$$

where J is the annular gap between displacer and cylinder (m), k_{pis} is the piston thermal conductivity ($W\,m^{-1}\,K^{-1}$), D_d is the displacer diameter (m), L_d is the displacer length (m), Z is the displacer stroke (m), T_d and T_c are, respectively, the temperature in the expansion space and in the compression space (K).

3. Mathematical background

There are many different ways to degrade the power produced by an ideal machine and to accurately predict power and efficiency requires an understanding of the design compartments.

Mathematical model takes into consideration different losses and pressure drop in heat exchangers.

Heat transfer and flow friction in the heat exchangers, i.e. the heater, the cooler and the regenerator, are evaluated using empirical equations under steady flow condition.

No leakage is allowed either through the appendix gap or through the seals of the connecting rods.

The temperature distribution in the various engine compartments is illustrated in Fig. 1(b).

The gas temperature in the various engine compartments is variable.

The cooler and the heater walls are maintained isothermally at temperatures T_{paf} and T_{pah}.

The pressure distribution is shown in Fig. 2.

The gas temperature in the different compartments is calculated according to the perfect gas law:

$$T_c = \frac{P_c V_c}{Rm_c}, \quad (12)$$

$$T_f = \frac{P_f V_f}{Rm_f}, \quad (13)$$

$$T_h = \frac{P_h V_h}{Rm_h}, \quad (14)$$

$$T_d = \frac{P_d V_d}{Rm_d}. \quad (15)$$

The regenerator is divided into two cells r1 and r2, each cell is been associated with its respective mixed mean gas temperature T_{r1} and T_{r2} expressed as follows:

$$T_{r1} = \frac{P_{r1} V_{r1}}{Rm_{r1}}, \quad (16)$$

$$T_{r2} = \frac{P_{r2} V_{r2}}{Rm_{r2}}. \quad (17)$$

An extrapolated linear curve is drawn through temperature values T_{r1} and T_{r2} defining the regenerator interface temperature T_{r-f} , T_{r-r} and T_{r-h}, as follows [12]:

$$T_{r-f} = \frac{3T_{r1} - T_{r2}}{2}, \quad (18)$$

$$T_{r-r} = \frac{T_{r1} + T_{r2}}{2}, \quad (19)$$

$$T_{r-h} = \frac{3T_{r2} - T_{r1}}{2}. \quad (20)$$

According to the flow direction of the fluid, the interface's temperatures: T_{c-f} , T_{f-r} , T_{r-h} and T_{h-d} are defined as follows [13]:

if $\dot{m}_{c-f} > 0$, then $T_{c-f} = T_c$, otherwise $T_{c-f} = T_f$,

if $\dot{m}_{f-r} > 0$, then $T_{f-r} = T_f$, otherwise $T_{f-r} = T_{r-f}$,

if $\dot{m}_{r-h} > 0$, then $T_{r-h} = T_{r-h}$, otherwise $T_{r-h} = T_h$,

if $\dot{m}_{h-d} > 0$, then $T_{h-d} = T_h$, otherwise $T_{h-d} = T_d$,

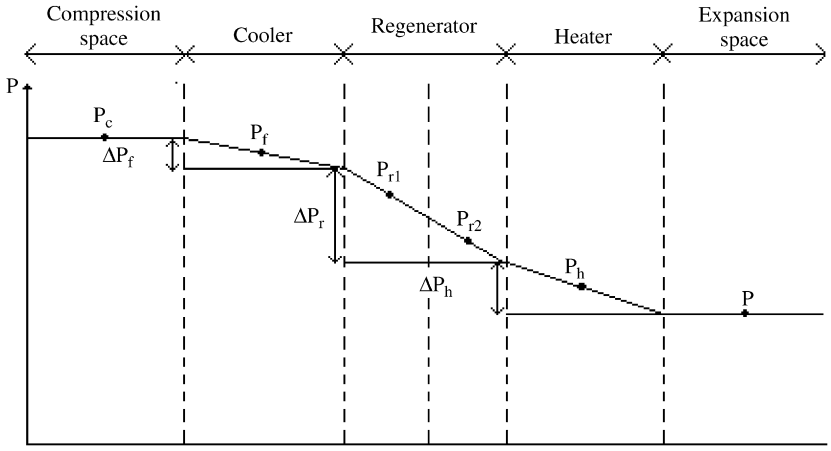

Fig. 2. Pressure distribution.

where T_{c-f} is the temperature of the interface between the compression space and the cooler, T_{f-r} is the temperature of the interface between the cooler and the regenerator, T_{r-h} is the temperature of the interface between the regenerator and the heater, T_{h-d} is the temperature of the interface between the heater and the expansion space.

The matrix temperatures are so given by

$$\frac{dT_{par1}}{dt} = -\frac{dQ_{r1}}{C_{pr}\,dt}, \tag{21}$$

$$\frac{dT_{par2}}{dt} = -\frac{dQ_{r2}}{C_{pr}\,dt}, \tag{22}$$

where C_{pr} is the heat capacity of each cell matrix ($J\,K^{-1}$), Q_{r1} is the quantity of heat exchanged to the regenerator r1 (j), Q_{r2} is the quantity of heat exchanged to the regenerator r2 (j), T_{Par1} is the matrix temperature in the regenerator r1 (K) and T_{Par2} is the matrix temperature in the regenerator r2 (K).

By taking into account the conduction loss in the exchangers and the regenerator effectiveness, the power exchanged in the different exchangers is written

$$d\dot{Q}_f = h_f A_{paf}(T_{paf} - T_f) - d\dot{Q}_{Pcdf}, \tag{23}$$

$$d\dot{Q}_{r2} = Eh_{r2}A_{par2}(T_{par2} - T_{r2}) - \frac{d\dot{Q}_{Pcdr2}}{2}, \tag{24}$$

$$d\dot{Q}_{r1} = Eh_{r1}A_{par1}(T_{par1} - T_{r1}) - \frac{d\dot{Q}_{Pcdr1}}{2}, \tag{25}$$

$$d\dot{Q}_h = h_h A_{pah}(T_{pah} - T_h) - d\dot{Q}_{Pcdh}, \tag{26}$$

where $d\dot{Q}_{Pcdh}$ is the conduction loss in the cooler (W), $d\dot{Q}_{Pcdr1}$ is the conduction loss in the regenerator r1 (W), $d\dot{Q}_{Pcdr2}$ is the conduction loss in the regenerator r2 (W) and $d\dot{Q}_{Pcdh}$ is the conduction loss in the heater (W).

The heat transfer coefficient of exchanges h_f, h_{r1}, h_{r2} and h_h is only available empirically [14].

The total exchanged heat is

$$d\dot{Q} = d\dot{Q}_f + d\dot{Q}_{r1} + d\dot{Q}_{r2} + d\dot{Q}_h - d\dot{Q}_{Pshtl}. \tag{27}$$

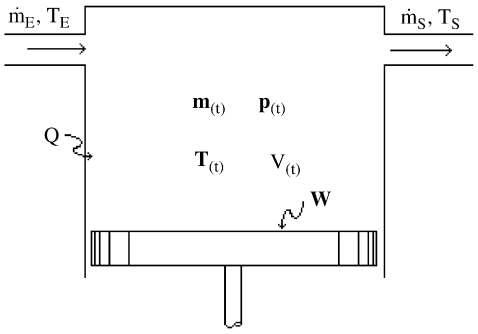

Fig. 3. Generalised cell.

The work given by the cycle is

$$\frac{dW}{dt} = P_c\frac{dV_c}{dt} + P_d\frac{dV_d}{dt}. \tag{28}$$

The thermal efficiency given by the cycle is:

$$\eta = \frac{W}{Q_h}. \tag{29}$$

The total engine volume is: $V_T = V_c + V_f + V_{r1} + V_{r2} + V_h + V_d$.

The other variables of the dynamic model are given by energy and mass conservation equation, applied to a generalised cell as follows (Fig. 3):

- Energy conservation equation :

$$d\dot{Q} + C_p T_E \dot{m}_E - C_p T_S \dot{m}_S = P\frac{dV}{dt} + C_v\frac{d(mT)}{dt}. \tag{30}$$

Since there is a variable pressure distribution throughout the engine, we have arbitrarily chosen the compression space pressure P_c as the baseline pressure. Thus, at each increment of the solution, P_c will be evaluated from the relevant differential equation and the pressure distribution is determined with respect to P_c. Thus it can be obtained

from the following expression:

$$P_f = P_c + \frac{\Delta P_f}{2}, \tag{31}$$

$$P_{r1} = P_f + \frac{(\Delta P_f + \Delta P_{r1})}{2}, \tag{32}$$

$$P_{r2} = P_{r1} + \frac{(\Delta P_{r1} + \Delta P_{r2})}{2}, \tag{33}$$

$$P_h = P_{r2} + \frac{(\Delta P_{r1} + \Delta P_h)}{2}, \tag{34}$$

$$P_d = P_h + \frac{\Delta P_h}{2}. \tag{35}$$

Applying energy conservation equation to the different engine cells, we obtain:

$$-C_p T_{c-f} \dot{m}_{cS} = \frac{1}{R}\left(C_p P_c \frac{dV_c}{dt} + C_v V_c \frac{dP_c}{dt}\right), \tag{36}$$

$$d\dot{Q}_f - d\dot{Q}_{pchf} + C_p T_{c-f}\dot{m}_{fE} - C_p T_{f-r}\dot{m}_{fS} = \frac{C_v V_f}{R}\frac{dP_c}{dt}, \tag{37}$$

$$d\dot{Q}_{r1} - d\dot{Q}_{Pchr1} + C_p T_{f-r}\dot{m}_{r1E} - C_p T_{r-r}\dot{m}_{r1S} = \frac{C_v V_{r1}}{R}\frac{dP_c}{dt}, \tag{38}$$

$$d\dot{Q}_{r2} - d\dot{Q}_{Pchr2} + C_p T_{r-r}\dot{m}_{r2E} - C_p T_{r-h}\dot{m}_{r2S} = \frac{C_v V_{r2}}{R}\frac{dP_c}{dt}, \tag{39}$$

$$d\dot{Q}_h - d\dot{Q}_{Pchh} + C_p T_{r-h}\dot{m}_{hE} - C_p T_{h-e}\dot{m}_{hS} = \frac{C_v V_h}{R}\frac{dP_c}{dt}, \tag{40}$$

$$C_p T_{h-d}\dot{m}_d - d\dot{Q}_{Pshtl} = \frac{1}{R}\left(C_p P_d \frac{dV_d}{dt} + C_v V_d \frac{dP_c}{dt}\right). \tag{41}$$

Summing Eqs. (36)–(41) we obtain the pressure variation:

$$\frac{dP_c}{dt} = \frac{1}{C_v V_T}\left[R(d\dot{Q} - d\dot{Q}_{PchT}) - C_p \frac{\delta W}{dt}\right]. \tag{42}$$

- Mass conservation equation:

$$M = m_d + m_c + m_f + m_r + m_h. \tag{43}$$

The mass flow in the different engine compartments is given by the energy conservation Eqs. (36)–(41):

$$\dot{m}_{cS} = -\frac{1}{RT_{c-f}}\left(P\frac{dV_c}{dt} + V_c\frac{dP_c}{\gamma dt}\right), \tag{44}$$

$$\dot{m}_{fS} = \frac{1}{C_p T_{f-r}}\left(d\dot{Q}_f - d\dot{Q}_{Pchf} + C_p T_{c-f}\dot{m}_{fE} - \frac{C_v V_f}{R}\frac{dP_c}{dt}\right), \tag{45}$$

$$\dot{m}_{r1S} = \frac{1}{C_p T_{r-r}}\left(d\dot{Q}_{r1} - d\dot{Q}_{Pchr1} + C_p T_{f-r}\dot{m}_{r1E} - \frac{C_v V_{r1}}{R}\frac{dP_c}{dt}\right), \tag{46}$$

$$\dot{m}_{r2S} = \frac{1}{C_p T_{r-h}}\left(d\dot{Q}_{r2} - d\dot{Q}_{Pchr2} + C_p T_{r-r}\dot{m}_{r2E} - \frac{C_v V_{r2}}{R}\frac{dP_c}{dt}\right), \tag{47}$$

$$\dot{m}_{hS} = \frac{1}{C_p T_{h-d}}\left(d\dot{Q}_h - d\dot{Q}_{Pchh} + C_p T_{r-h}\dot{m}_{hE}\frac{dm_h}{dtE} - \frac{C_v V_h}{R}\frac{dP_c}{dt}\right), \tag{48}$$

where: $\dot{m}_{cS} = \dot{m}_{fE}$; $\dot{m}_{fS} = \dot{m}_{r1E}$; $\dot{m}_{r1S} = \dot{m}_{r2E}$; $\dot{m}_{r2S} = \dot{m}_{hE}$ and $\dot{m}_{hS} = \dot{m}_{dE}$.

3.1. Solution method

The systems of differential equations are written as follows:

$$dY = F(t, y),$$

$$Y(t_0) = Y_0,$$

Y is a vector representing the unknown of each system, $Y(t_0) = Y_0$ is the initial condition.

These systems of equations are solved by the classical fourth-order Runge–Kutta method, cycle after cycle until steady.

4. Design specification and concept

4.1. Engine specification

The engine parameters should be optimised [15] to avoid losses and to obtain high thermal efficiency for all the engine components especially heat exchangers. While the main target of the engine is to produce sufficient power to run a connecting application, there are conditions which pose critical constraints on the design, the working fluid is hydrogen and the temperature difference between the heater and the cooler is about 300 °C only.

The engine presented in Fig. 4 uses a conventional crank mechanism driving two pistons by means of yoke linkage. The major feature of this is that there is almost no lateral movement of the connecting rods resulting in very small side forces on the pistons. With the lack of lateral movement of the connecting rods, there are relatively large unbalanced lateral forces due to the crankshaft counterweight. Ross has a patented gear mechanism which balances the lateral forces by splitting and counter-rotating the counterweight

4.2. Design concept

The yoke drive mechanism does not produce sinusoidal volume variations and the exact piston displacement functions are extremely complex. The volume variations

are derived from geometric considerations in Fig. 5 and Table 1.

The main Design concepts are listed in Table 2.

5. Design analyses

5.1. Relationship for engine power, swept volumes and dead volumes

The purpose of this simulation is to estimate the main volumes of the engine spaces in terms of swept volumes and

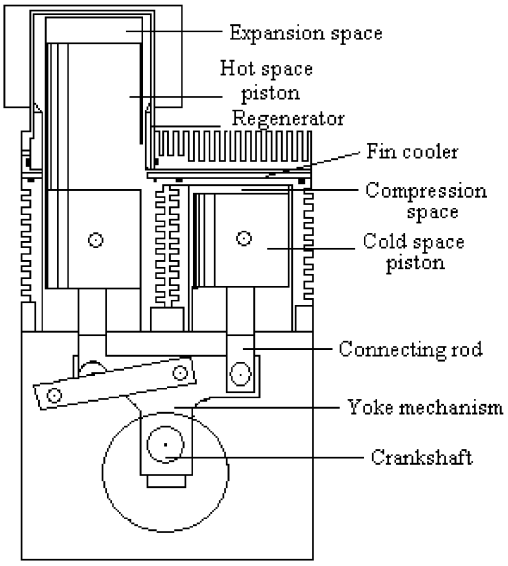

Fig. 4. The Ross Yoke drive engine—schematic cross section view.

Table 1
Volumes variations

Geometrical parameters	$b_1 = \sin\varphi = r\cos\theta$ $b_\theta = \sqrt{b_1^2 - (r\cos\theta)^2}$ $X = r\sin\theta + b_\theta$
Displacements	$Y_c = r[\sin\theta - \cos\theta(b_2/b_1)] + b_\theta$ $Y_e = r[\sin\theta + \cos\theta(b_2/b_1)] + b_\theta$
Volume variations	$V_c = V_{mc} + A_P(Y_{max} - Y_c)$ $V_e = V_{me} + A_d(Y_{max} - Y_\theta)$
$\frac{dV_c}{d\theta} = A_p r\left[\cos\theta + \sin\theta\left(\frac{b_2}{b_1}\right) + \frac{r\sin\theta\cos\theta}{b_\theta}\right]$	
$\frac{dV_e}{d\theta} = A_d r\left[\cos\theta - \sin\theta\left(\frac{b_2}{b_1}\right) + \frac{r\sin\theta\cos\theta}{b_\theta}\right]$	

Table 2
Concepts and target performance

Parameters	Values/type
Engine type	Alpha
Working fluid	Hydrogen
Crank length	$r = 7.6$ mm
Yoke crank length	$b_1 = 29$ mm
Piston length	$b_2 = 29$ mm
Displacement extremities	$Y_{min} = 17.75$ mm $Y_{max} = 39.28$ mm
Mean phase angle advance	$\alpha = 90^\circ$
Mass of gas in engine	$M = 0.35$ g
Hot space temperature	$T_h = 590$ K
Cold space temperature	$T_k = 290$ K
Frequency	Freq = 41.72 Hz

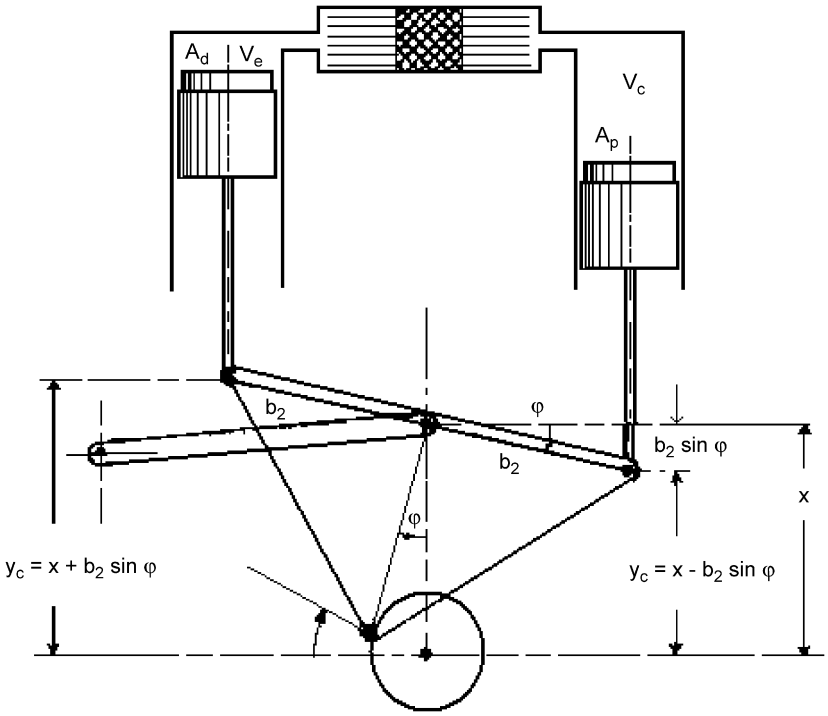

Fig. 5. Geometric derivation of the Ross Yoke drive equation.

dead volumes using Dynamic model with losses since these factors are essential in estimating the preliminary configuration of the engine and will influence the subsequent optimisation process. Since it has been decided to adopt the successive alpha-type Ross Yoke configuration, the compression swept volume V_c should be equal to the expansion swept volume V_d, and thus the swept volume ratio $k = V_c/V_d$.

In addition, at this stage, it is assumed that the mean pressure of the engine during operation is of 8.7 bar, which is the kind of pressure which normally occurs before the engine start-up. It is obvious from dynamic model equations that the net cycle power and the thermal load on the heat exchangers are direct linear functions of the engine speed (Operating rotation), the maximum pressure of the working fluid and the size of the engine, which is expressed in term of the swept volume [16]. However, the direct effects of the dead volume and swept volume to the engine power should be detailed. Figs. 6 and 7 illustrates the variation of the power as a function of the swept volume, which was calculated on the dead volumes of 535 and 370 cm^3 under the fixed temperature difference of 300 °C. It is shown that the power increases when the swept volume increases until an optimal value. Also, it is noticeable that the power increases with the increase in speed. These two remarks imply that we have an optimal value of swept volume for maximum engine power for several speeds. By comparing the two graphs in Figs. 6 and 7, based on the same swept volume, it can be said that the decrease in dead volume will lead to an increase in engine power.

To illustrate the effect of the dead volume clearly, the variation of the engine power as a function of dead volume is calculated and the results are as shown in Figs. 8 and 9 for the operating frequency of 75 and 35 Hz.

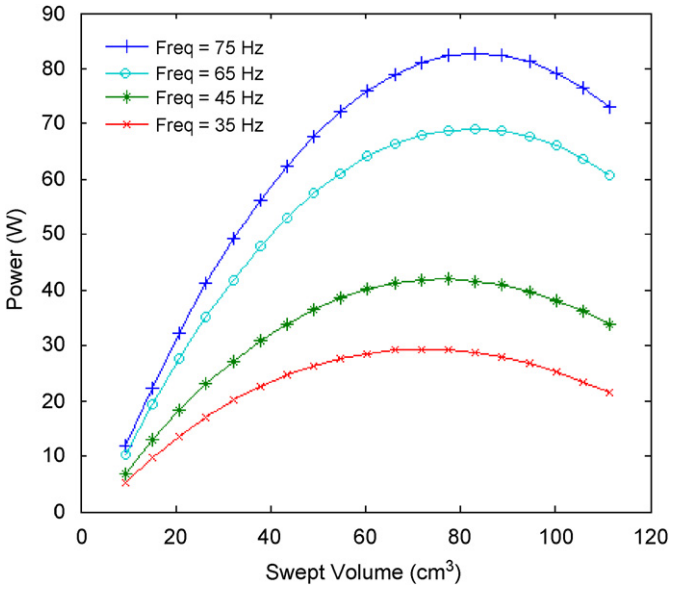

Fig. 6. Relationship between swept volume and engine power (dead volume 535 cm^3).

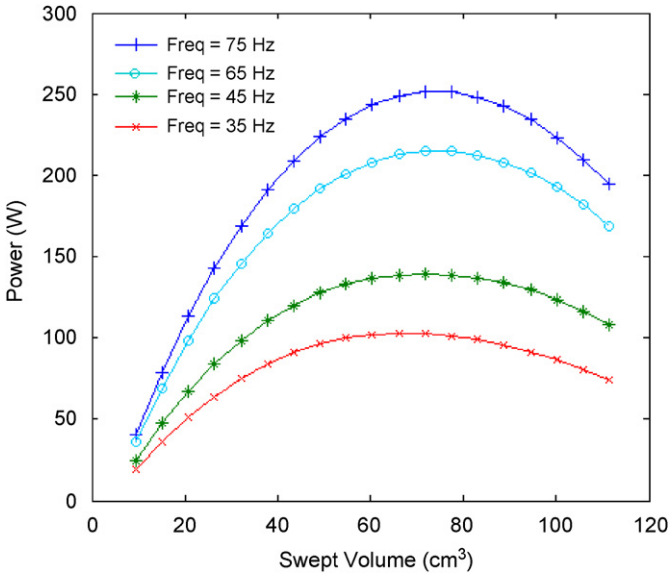

Fig. 7. Relationship between swept volume and engine power (dead volume 370 cm^3).

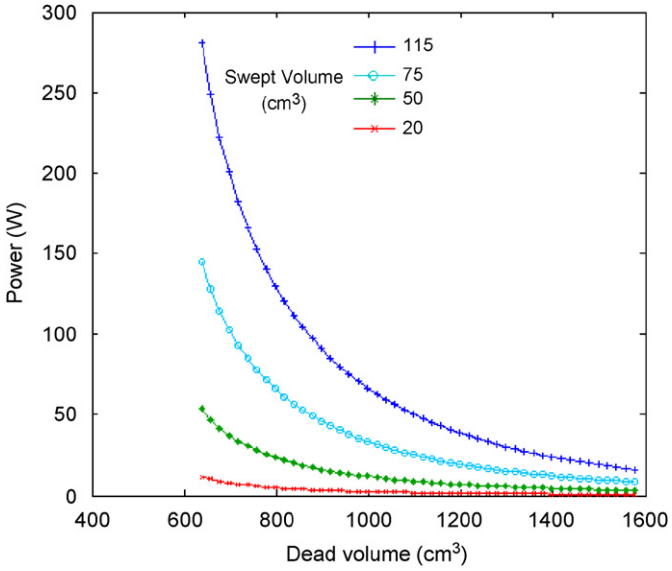

Fig. 8. Relationship between dead volume and engine power (frequency = 75 Hz).

From Figs. 6–9, it can be seen that the increase in the dead volume produces an exponential drop in the net power, which in turn decreases the maximum pressure. However, the calculation is performed under the assumption that the temperature difference is 300 °C, which can be obtained from the solar system with average concentration.

5.2. Relationship for heater and cooler parameters

An important factor in heat exchanger design is volume. Cooler and heater volumes contribute to large portions of dead volume. Previous studies showed that the dead volumes, which includes those in the heat exchangers, is

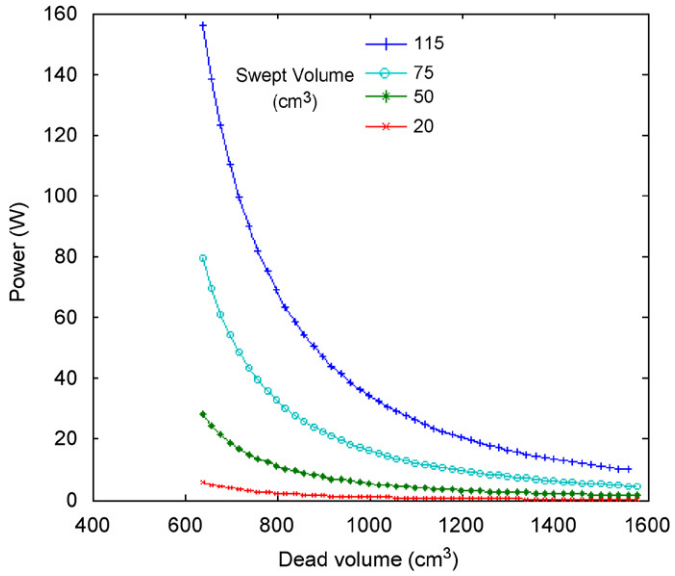

Fig. 9. Relationship between dead volume and engine power (frequency = 35 Hz).

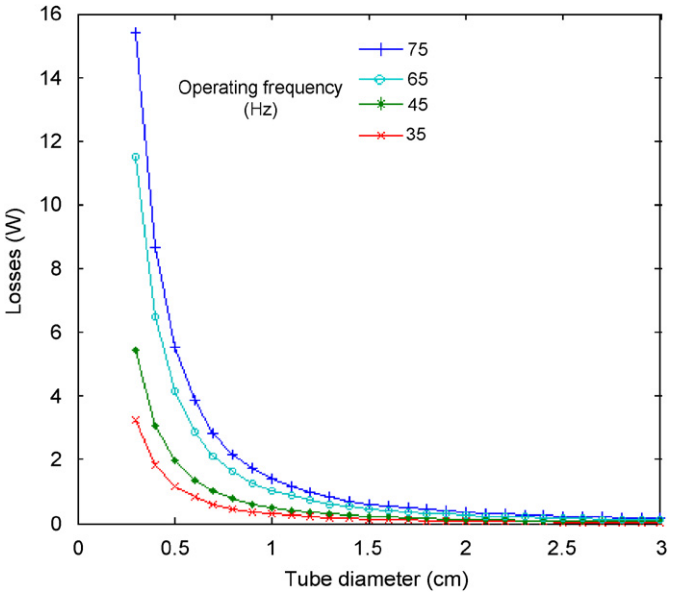

Fig. 10. Relationship of heater tube diameters with the friction losses (swept volume = 75 cm^3, tube length = 0.45 m, cooler volume 165 cm^3).

an essential factor in the Stirling engine design, where it should be small as possible [17]. To demonstrate the relationships for the heaters, specific conditions of 75 cm^3 swept volume and 0.45 m tube length are used.

After carrying out thermodynamic simulation for the heater, the variation of its tube diameter can be derived as a function of friction losses for several values of engine speeds as being depicted in Fig. 10 for the heater volume of 165 cm^3. Similarly, Fig. 11 shows the graphs for the heater volume of 80 cm^3. Both graphs indicate an inverse proportionality between tube diameter and friction loss in the heater. The explanation of this variation is that the tube with smaller diameter having the same length delivers the same mass flux, thus generates a shorter entrance length and a thicker viscous boundary layer, which then leads to a higher friction factor of the flow. For the cooler, by using the same values for swept volume and tube length, the equivalent graphs for the cooler volumes of 165 and 80 cm^3 are shown in Figs. 12 and 13, which indicates a similar pattern to that of the heater.

In designing heat exchangers, an important consideration for the heat exchangers is to have an ability to supply or reject the required amount of heat to or from the engine. In this aspect, one crucial factor is the heat transfer area, which will decide the amount of heat energy to be transported. Hence, in order to achieve a high effectiveness for the heater and the cooler, larger transfer areas, and thus larger volumes, are needed.

5.3. Relationship for regenerator parameters

The effect of pressure drop in the regenerator of a mean temperature differential Stirling engine to thermal efficiency is very important since it can decrease the overall efficiency of the engine [16,17]. To analyse this effect and its

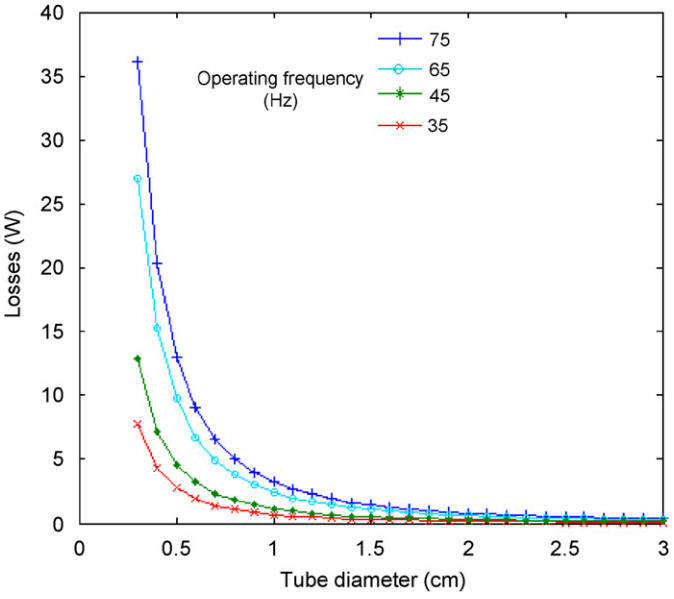

Fig. 11. Relationship of heater tube diameters with the friction losses (swept volume = 75 cm^3, tube length = 0.45 m, cooler volume 80 cm^3).

implication to the efficiency of the engine, six types of matrices has been selected and is being subjected to various pressure drops and engine speeds. The configurations for these six matrices are given in Table 3 for a standard total wire length of 5 m. The porosity of each matrix is important since it will have a direct impact on the performance of the regenerator, and can be determined by its geometry, namely, wire diameter, density of the mesh and the void volume. Any changes in the porosity will also change the regenerator effectiveness and the pressure drop, which eventually affects the engine efficiency. Therefore, the best matrix for the regenerator should possess both high efficiency and low-pressure drop.

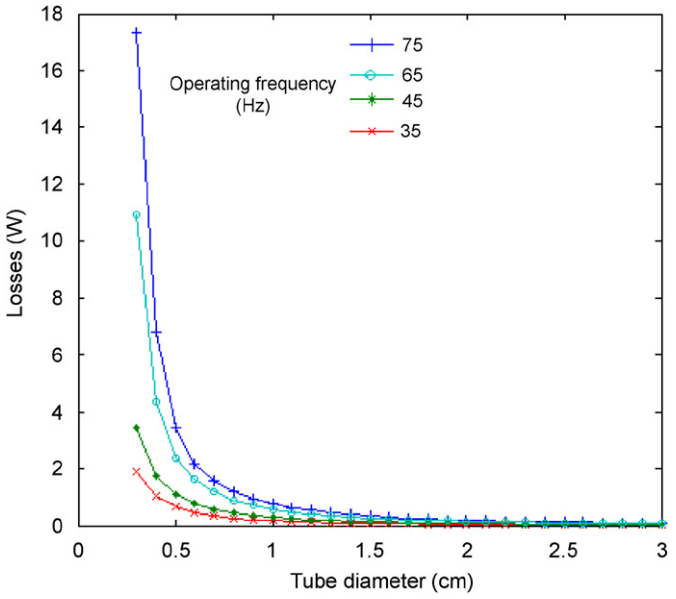

Fig. 12. Relationship of cooler tube diameters with the friction losses (swept volume = 75 cm^3, tube length = 0.45 m, heater volume 165 cm^3).

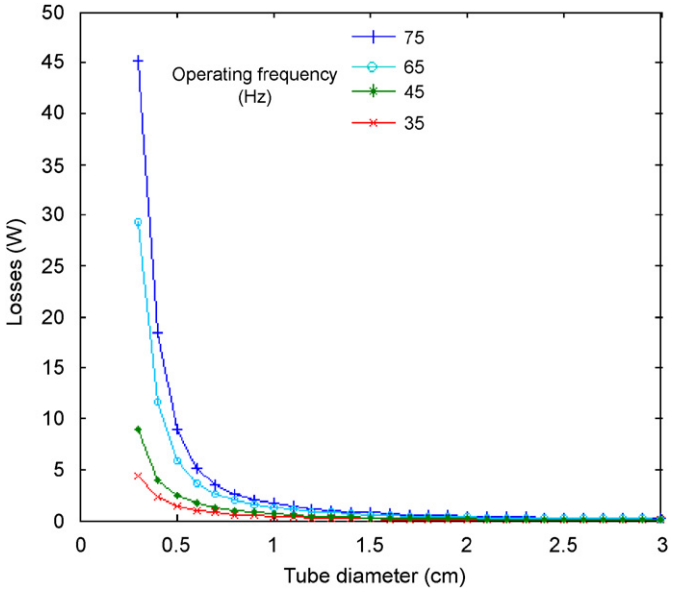

Fig. 13. Relationship of cooler tube diameters with the friction losses (swept volume = 75 cm^3, tube length = 0.45 m, heater volume 80 cm^3).

Fig. 14 shows the relationship between the operating frequency and the pressure drop for these matrices. The pressure drop is found to be proportional to the frequency since an increase in frequency increases the mass flux through the regenerator as well as the pressure magnitude up to the same proportion for the same matrices. On the other hand, the decrease in mesh porosity leads to the higher friction factor as well as increases the pressure drop. Hence, it can be said that M1 has a lowest pressure drop in comparison to the others at a same speed because its porosity is the highest. In order to obtain a higher porosity, and thus the lower pressure drop, the meshes should be made from small wire diameter and should be as coarse as possible. However, the pressure drop in the regenerator alone is not sufficient in deciding the best regenerator without considering its heat transfer behaviour. But Table 4 shows the relationship between the thermal efficiency, power of the engine and matrix type. The best matrix should compromise between high effectiveness and low-pressure drop in order to obtain minimal losses in the regenerator, and in this case, M6 with the porosity of 0.6112 and wire diameter 0.009 m has been chosen for the design.

The decrease in mesh porosity leads to the higher friction factor as well as increases the pressure drop. Hence, it can be said that M1 has a lowest pressure drop in comparison to the others at a same frequency because its porosity is the highest. In order to obtain a higher porosity, and thus the lower pressure drop, the meshes should be made from small wire diameter and should be as coarse as possible. However, the pressure drop in the regenerator alone is

Table 3
Geometrical properties of wire mesh for regenerator

Matrix	Wire diameter (m)	Porosity (ψ)
M1	0.0035	0.9122
M2	0.0050	0.8359
M3	0.0065	0.7508
M4	0.0070	0.7221
M5	0.0080	0.6655
M6	0.0090	0.6112

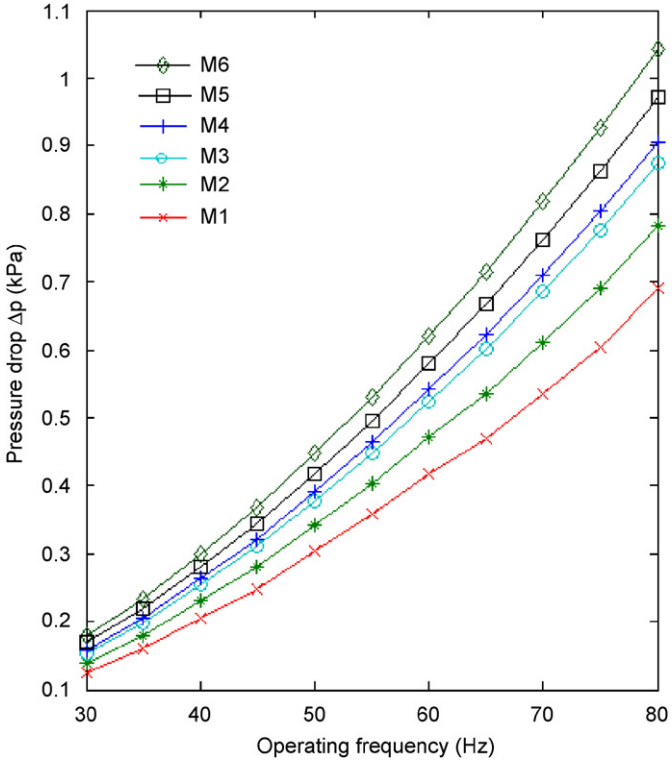

Fig. 14. Relationship between pressure drop and operating frequency.

Table 4
Effect of matrix on power and thermal efficiency

Matrix	Power (W)	Thermal efficiency (%)
M1	159.39	10.79
M2	226.42	22.41
M3	249.20	33.90
M4	252.50	37.32
M5	255.92	43.32
M6	256.77	48.11

not sufficient in deciding the best regenerator without considering its heat transfer behaviour this is the case of M6 In spite of the higher pressure drop we have better power and thermal efficiency because we have better heat transfer.

The regenerator effectiveness ε can be manipulated by varying wire diameter and wire length, which in turn changes the "wetted" surface area. It can be represented in form of the relationship between the porosity or the number of transfer units (NTU) and the thermal heating efficiency of the engine. If the wetted surface area is large, the resulting porosity should be low, and this provides the air or the work fluid with a large contacting surface to achieve a high rate of heat transfer. Hence, the NTU, and thus ε, are increased when the surface area increases. The effect of ε on the thermal efficiency of the engine is that it represents the ability to reject the heat to the working gas when the gas exits through the heater and the ability to absorb the heat when the gas exits through the cooler.

6. Conclusion

In this paper, a number of technical considerations in designing a mean temperature differential Stirling engine have been proposed. These considerations have been established through the use of the dynamic model with losses energy and pressure drop in heat exchangers. As a result, the optimal configuration for the design can be summarised as follow.

- This studies show clearly that, for given value of difference temperature, operating frequency and dead volume there is a definite optimal value of swept volume ratio at which the power is a maximum. In this paper, the optimal swept volume is $75\,cm^3$ for frequency = 75 Hz.
- Upon optimisation, operating frequency has to be limited between 35 and 75 Hz at a temperature difference of 300 °C, where the best value is 75 Hz.
- For the regenerator, its porosity plays a significant role in controlling pressure drop of the regenerator, which can be manipulated by varying wire diameter and length. For this engine, the selected parameters are the wire diameter of 3.5 mm with a total length of 5 m and a porosity of 0.9122 to have low pressure drop but in our case M6 give the best thermal efficiency of the engine.
- The heat exchanger volumes should be evaluated by considering both the pressure drop and the thermal efficiency of the engine. In our case the optimal heat exchanger volume has been found to be $165\,cm^3$ for both the cooler and the tube dimension is 0.011 m in diameter and 0.450 m in length.

References

[1] Kongtragool B, Wongwises S. A review of solar-powered Stirling engines and low temperature differential Stirling engines. Renewable Sustainable Energy Rev 2003;7:131–54.

[2] Bonnet S, Alaphilippe M, Stouffs P. Conversion thermodynamique de l'energie solaire dans des installations de faible ou de Moyenne Puissance: réflexions sur le Choix du Meilleur Degré de concentration. Rev Energ Ren 11èmes Journées Int Therm 2003; 73–80.

[3] Berchowitz DM, Urieli I. Stirling cycle engine analysis. Bristol: Adam Hilger Ltd; 1984.

[4] Timoumi Y, Ben Nasrallah S. Design and fabrication of a Stirling–Ringbom engine running at a low temperature. In: TSS international conference in mechanics and engineering (ICAME) March, Hammamet, Tunisia; 2002.

[5] Park SJ, Hong YJ, Kim HB, Lee KB. An experimental study on the phase shift between piston and displacer in the Stirling cryocooler. Curr Appl Phys 2003;3:449–55.

[6] Capeto C, Rispoli F. New drive mechanisms for the Stirling engine' 8th international Stirling engine conference and exhibition, May 27–30, Ancona; 1997. p. 39–49.

[7] Bartczak L, Carlsen H, An optimization study of Stirling engines based on advanced simulation. In: Proceedings, 5th international Stirling engine conference. Dubrovnik; 1991. p. 161–6.

[8] Kolin I. Stirling motor: history-theory-practice. Dubrovnik: Inter University Center; 1991.

[9] James RS. Ringbom Stirling engines. New York: Oxford University Press; 1985.

[10] Tlili S. Modélisation des moteurs Stirling, DEA, Ecole National d'Ingénieurs de Monastir. Tunisie; 2002.

[11] Tlili S, Timoumi Y. Numerical simulation and losses analysis in a Stirling engine. Int J Heat Tech 2006;24(1):97–103.

[12] Poncet E, Nika P, Béreiziat D, Lanzetta F. Technique de caractérisation d'un mini-régénérateur thermique pour mini-refroidisseur Stirling ou tube à gaz pulsé'. Méc Ind 2001;2(5):455–64.

[13] Popescu G, Radcenco V, Costea M, Feidt M. Optimisation thermodynamique en temps fini du moteur de Stirling endo- et exo-irréversible. Rev Gén Therm 1996;35:656–61.

[14] Walker G. Stirling engines. Oxford: Clarendon Press; 1980.

[15] Halit K, Huseyin S, Atilla K. Manufacturing and testing of a V-type Stirling engine. Turk J Engine Environ Sci 2000;24:71–80.

[16] Organ AJ. The regenerator and the Stirling engine. Mechanical Engineering Publications; 1997.

[17] Ataer OE. Numerical analysis of regenerators of piston type Stirling engines using Lagrangian formulation. Int J Refrig 2002;25:640–52.p, c_{pr} and c_v has been changed to C_p, C_{pr} and C_v respectively.>